

The Functional Specialization of Exomer as a Cargo Adaptor During the Evolution of Fungi

Carlos Anton,* Javier Valdez Taubas,[†] and Cesar Roncero*¹

*Departamento de Microbiología y Genética, Instituto de Biología Funcional y Genómica, Consejo Superior de Investigaciones Científicas-Universidad de Salamanca, 37007, Spain and [†]Departamento de Química Biológica, Centro de Investigaciones en Química Biológica de Córdoba, Consejo Nacional de Investigaciones Científicas y Técnicas, Facultad de Ciencias Químicas, Universidad Nacional de Córdoba, X5000HUA Argentina

ORCID IDs: 0000-0002-7497-0080 (C.A.); 0000-0001-5964-3252 (C.R.)

ABSTRACT Yeast exomer is a heterotetrameric complex that is assembled at the *trans*-Golgi network, which is required for the delivery of a distinct set of proteins to the plasma membrane using ChAPs (Chs5-Arf1 binding proteins) Chs6 and Bch2 as dedicated cargo adaptors. However, our results show a significant functional divergence between them, suggesting an evolutionary specialization among the ChAPs. Moreover, the characterization of exomer mutants in several fungi indicates that exomer's function as a cargo adaptor is a late evolutionary acquisition associated with several gene duplications of the fungal ChAPs ancestor. Initial gene duplication led to the formation of the two ChAPs families, Chs6 and Bch1, in the Saccharomycotina group, which have remained functionally redundant based on the characterization of *Kluyveromyces lactis* mutants. The whole-genome duplication that occurred within the *Saccharomyces* genus facilitated a further divergence, which allowed Chs6/Bch2 and Bch1/Bud7 pairs to become specialized for specific cellular functions. We also show that the behavior of *S. cerevisiae* Chs3 as an exomer cargo is associated with the presence of specific cytosolic domains in this protein, which favor its interaction with exomer and AP-1 complexes. However, these domains are not conserved in the Chs3 proteins of other fungi, suggesting that they arose late in the evolution of fungi associated with the specialization of ChAPs as cargo adaptors.

KEYWORDS evolution; exomer; intracellular traffic; yeast

THE *trans*-Golgi network (TGN) constitutes a major sorting platform for the intracellular trafficking of proteins in all eukaryotic cells (Guo *et al.* 2014); therefore, it is not surprising that the molecular mechanisms involved in protein sorting at the TGN are evolutionarily conserved. However, despite this conservation, very little is known about the mechanisms that participate in this event.

Chitin synthesis in yeast was envisioned several years ago as a model for the study of the intracellular trafficking of proteins because the activity of the major chitin synthase depends on the efficient traffic of its catalytic subunit, Chs3, to the plasma membrane (PM) (Roncero 2002). In *Saccharomyces cerevisiae*,

the trafficking of Chs3 to the PM is blocked at the TGN/EE boundary in the absence of Chs5 (Santos and Snyder 1997) or Chs6 (Ziman *et al.* 1998) proteins. A further characterization of these proteins showed that both form the exomer together with three Chs6 paralogs, a complex that is required for the TGN to cell surface transport of Chs3 (Santos and Snyder 1997; Sanchatjate and Schekman 2006; Trautwein *et al.* 2006; Wang *et al.* 2006). Later on, it was demonstrated that the proteins Fus1 (Santos and Snyder 2003; Barfield *et al.* 2009) and Pin2 (Ritz *et al.* 2014) also depend on exomer for their delivery to the PM. Fus1 and Pin2 are proteins that contain a single transmembrane (TM) domain with very different functions; while Fus1 is required for cell fusion during mating (Trueheart *et al.* 1987), Pin2 is a prion-inducing protein (Ritz *et al.* 2014). Despite their different secondary structures and functions, these three proteins are fully retained at the TGN in the absence of exomer and have thus been described as *bona fide* exomer cargos. Accordingly, exomer is currently described as a specialized sorting platform at the TGN (Spang 2015).

Copyright © 2018 by the Genetics Society of America

doi: <https://doi.org/10.1534/genetics.118.300767>

Manuscript received November 6, 2017; accepted for publication January 31, 2018; published Early Online February 6, 2018.

Supplemental material is available online at <http://www.genetics.org/lookup/suppl/doi:10.1534/genetics.118.300767/-/DC1>.

¹Corresponding author: Consejo Superior de Investigaciones Científicas-Universidad de Salamanca, Instituto de Biología Funcional y Genómica, C/Zacarias González, 37007 Salamanca, Spain. E-mail: crm@usal.es

Exomer is assembled at the TGN as a heterotetrameric complex formed by a dimer of *Chs5* bound to two other molecules of either *Bch1*, *Bud7*, *Chs6*, or *Bch2* (Paczkowski *et al.* 2012), all members of the ChAPs (*Chs5*-*Arf1* binding proteins) family (Trautwein *et al.* 2006). This complex interacts directly with the *Arf1* GTPase through both *Chs5* and ChAPs components (see Supplemental Material, Figure S1 in File S1 for a model of exomer assembly). Based on sequence comparisons, ChAPs are separated into two groups: *Bch1/Bud7* and *Chs6/Bch2* (Trautwein *et al.* 2006). *Bch1* has been shown to have a defined role in the recruitment of the GTPase *Arf1* to the exomer and, consequently, influences the capacity of exomer to bend membranes *in vitro* (Paczkowski and Fromme 2014). Accordingly, *Bch1* is also the most efficient ChAPs in the functional assemblage of exomer (Huranova *et al.* 2016). *Bud7*, which to date is poorly characterized, probably has redundant functions with *Bch1* (Huranova *et al.* 2016). In contrast, *Chs6* does not seem to have any critical role in the assembly of exomer but acts as a dedicated exomer cargo adaptor. *Chs3* interacts with *Chs6* through its C- and N-terminal cytosolic regions (Rockenbauch *et al.* 2012; Weiskoff and Fromme 2014), facilitating its sorting at the TGN. Hence, in the absence of *Chs6*, *Chs3* is retained at the TGN. Interestingly, the concomitant absence of *Bch1/Bud7* also blocks *Chs3* at the TGN, which is most likely due to a general defect in the functioning of exomer (Paczkowski and Fromme 2014). The function of *Bch2*, the closest homolog to *Chs6*, is not understood, owing to the absence of distinct phenotypes for the single mutant *bch2Δ*. However, *Bch2* is possibly the cargo adaptor of *Pin2* (Ritz *et al.* 2014) and could also have a minor role in exomer assembly at the TGN (Huranova *et al.* 2016).

All of the *bona fide* cargos of exomer described so far share the additional characteristics of a polarized distribution and their arrival at the PM through an alternative route in the absence of any of the clathrin adaptor complexes AP-1, *Gga1/2*, or *Ent3/5*, which are known to regulate endocytic recycling (Valdivia *et al.* 2002; Copic *et al.* 2007; Barfield *et al.* 2009; Ritz *et al.* 2014). This poorly defined route allows the arrival of these cargos at the PM even in the absence of exomer. The mechanisms by which these cargos follow either route to the PM are not understood; however, it is known that a single mutation in the N-terminal domain of *Chs3*, L24A, triggers its transport via the alternative route by abolishing the physical interaction between *Chs3* and the AP-1 complex (Starr *et al.* 2012). The role of *Gga1/2* in this process is probably indirect, due to their early acting function, which recruits AP-1 for coat assembly at the TGN (Daboussi *et al.* 2012).

However, exomer mutants display several additional phenotypes (Trautwein *et al.* 2006) that cannot be linked to the defective transport of any of the exomer cargos described to date. Accordingly, our laboratory recently showed that the PM ATPase *Ena1* relies on exomer for its polarized transport under several forms of stress, although this protein effectively reaches the PM in the *chs5Δ* mutant (Anton *et al.* 2017). This finding suggests a potential role for exomer in the trafficking of a

higher number of proteins that are not recognized as *bona fide* exomer cargos. Moreover, the absence of exomer also affects *RIM101* signaling by altering the recruitment of the molecular machinery involved in the proteolytic processing of *Rim101*. These findings are consistent with exomer having a more general role in the organization of the TGN, which has been proposed following the characterization of exomer-deficient mutants in *Schizosaccharomyces pombe* (Hoya *et al.* 2017).

The basic rules governing intercellular trafficking are simple and relatively well conserved, but its complexity is enormous, providing specific solutions for the traffic between different organelles (Schlacht *et al.* 2014). Part of this complexity is achieved by the presence of multiple families of paralogous proteins that can act at discrete localizations or interact with different groups of cargos. Hence, the specificity of trafficking is in part encoded in the combinatorial interactions of these various players, including small GTPases and their regulators, cargo adaptors, and coat proteins. The functional relationship between exomer and several of the adaptor complexes described above, together with the evolutionary conservation of both complexes (Trautwein *et al.* 2006; Barlow *et al.* 2014) in fungi, provides an attractive framework for studying the potential coevolution between both complexes. Moreover, the evolutionary divergence of the ChAPs family provides the possibility of testing the potential specialization of exomer function along fungal evolution, while also addressing the ancient and conserved function of exomer.

Materials and Methods

Yeast strain construction

S. cerevisiae mutant strains were all made in the W303 background. *Kluyveromyces lactis* KHO69-8C, *Candida albicans* BWP17, and *Ustilago maydis* FB1 background strains were also used (Table 1). Specific transformation protocols were used for each species (see below).

***S. cerevisiae* constructions:** Yeast cells were transformed using the standard lithium acetate/polyethylene glycol procedure (Rose *et al.* 1990). Gene deletions were made using the gene replacement technique, with different deletion cassettes based on the *natMX4*, *kanMX4*, or *hphNT1* resistance genes (Goldstein and McCusker 1999). For the insertion of the *GAL1* promoter in front of the different ORFs, the cassette was amplified from pFA6a-*kanMX4*-p*GAL1* (Longtine *et al.* 1998). Proteins were tagged chromosomally at their C-terminus with GFP or mCherry, employing integrative cassettes amplified from pFA6a-GFP-*hphMx6*/pFA6a-GFP::*natMx4* or pFN21 (Sato *et al.* 2005). The *delitto perfetto* technique was performed to generate the gene truncations within the genome. In brief, this approach allows *in vivo* mutagenesis using two rounds of homologous recombination. The first step involves the insertion of a cassette containing two markers at or near the locus to be altered. The second one involves complete removal of the cassette and transfer of the expected genetic modification

Table 1 Yeast strains used

Strain	Genotype	Origin/reference
<i>S. cerevisiae</i>		
CRM67	W303, MATa, (<i>leu2-3,112 trp1-1 can1-100 ura3-1 ade2-1 his3-11,15</i>)	Laboratory collection
CRM2268	W303, MATa, <i>chs5Δ::natMx4</i>	Laboratory collection
CRM1590	W303, MATa, <i>chs3Δ::natMx4</i>	Laboratory collection
CRM1278	W303, MATa, <i>chs3Δ::URA3 chs5Δ::natMx4</i>	Laboratory collection
CRM2775	W303, MATa, <i>bch1Δ::kanMx4</i>	This study
CRM2778	W303, MATa, <i>bud7Δ::natMx4</i>	This study
CRM3068	W303, MATa, <i>chs6Δ::kanMx4</i>	This study
CRM3083	W303, MATa, <i>bch2Δ::natMx4</i>	This study
CRM3066	W303, MATa, <i>bch1Δ::kanMx4 bud7Δ::natMx4</i>	This study
CRM3081	W303, MATa, <i>chs6Δ::kanMx4 bch2Δ::natMx4</i>	This study
CRM2233	W303, MATa, <i>kanMx6::PGAL1-BCH1</i>	This study
CRM2244	W303, MATa, <i>kanMx6::PGAL1-BUD7</i>	This study
CRM2379	W303, MATa, <i>kanMx6::PGAL1-CHS6</i>	This study
CRM2426	W303, MATa, <i>kanMx6::PGAL1-BCH2</i>	This study
CRM1777	W303, MATa, <i>chs3Δ::URA3 aps1Δ::kanMx4</i>	Laboratory collection
CRM3089	W303, MATa, <i>bch1Δ::kanMx4 bud7Δ::natMx4 chs3Δ::hphNT1</i>	This study
CRM3091	W303, MATa, <i>chs6Δ::kanMx4 bch2Δ::natMx4 chs3Δ::hphNT1</i>	This study
CRM3155	W303, MATa, <i>aps1Δ::kanMx4</i>	Laboratory collection
CRM3157	W303, MATa, <i>chs5Δ::natMx4 aps1Δ::kanMx4</i>	Laboratory collection
CRM2406	W303, MATa, <i>PIN2-GFP::hphNT1</i>	Laboratory collection
CRM2507	W303, MATa, <i>chs5Δ::natMx4 PIN2-GFP::hphNT1</i>	Laboratory collection
CRM2474	W303, MATa, <i>kanMx6::PGAL1-BUD7 PIN2-GFP::hphNT1</i>	This study
CRM2509	W303, MATa, <i>kanMx6::PGAL1-BCH2 PIN2-GFP::hphNT1</i>	This study
CRM2511	W303, MATa, <i>kanMx6::PGAL1-BCH1 PIN2-GFP::hphNT1</i>	This study
CRM2512	W303, MATa, <i>kanMx6::PGAL1-BCH6 PIN2-GFP::hphNT1</i>	This study
CRM2287	W303, MATa, <i>bar1Δ::natMx4</i>	This study
CRM2461	W303, MATa, <i>bar1Δ::natMx4 chs5Δ:: hphNT1</i>	This study
CRM2288	W303, MATa, <i>kanMx6::PGAL1-BCH1 bar1Δ::natMx4</i>	This study
CRM2289	W303, MATa, <i>kanMx6::PGAL1-BUD7 bar1Δ::natMx4</i>	This study
CRM1821	W303, MATa, <i>CHS6-mCherry::natMx4</i>	Laboratory collection
CRM2179	W303, MATa, <i>CHS5-mCherry::natMx4</i>	Laboratory collection
CRM2235	W303, MATa, <i>BCH2-GFP::hphNT1</i>	This study
CRM2637	W303, MATa, <i>BCH2Δ¹¹⁸-GFP::natMx4</i>	This study
CRM2639	W303, MATa, <i>BCH2Δ³¹-GFP::natMx4</i>	This study
CRM2584	W303, MATa, <i>kanMx6::PGAL1-BCH1-BCH2^{Frg1}</i>	This study
CRM2586	W303, MATa, <i>kanMx6::PGAL1-BCH1-BCH2^{Frg2}</i>	This study
CRM2588	W303, MATa, <i>kanMx6::PGAL1-BCH1-BCH2^{Frg3}</i>	This study
CRM2641	W303, MATa, <i>kanMx6::PGAL1-BCH2-GFP::natMx4</i>	This study
CRM2644	W303, MATa, <i>kanMx6::PGAL1-BCH2Δ¹¹⁸-GFP::natMx4</i>	This study
CRM2647	W303, MATa, <i>kanMx6::PGAL1-BCH2Δ³¹-GFP::natMx4</i>	This study
<i>K. lactis</i>		
CRM2632	KHO69-8C, MATα, (<i>ura3 leu2 his3:loxP ku80:loxP</i>)	Heinisch et al. (2010)
CRM2823	KHO69-8C, MATα, <i>Klchs5Δ::URA3</i>	This study
CRM2666	KHO69-8C, MATα, <i>Klchs3Δ::LEU2</i>	This study
CRM2677	KHO69-8C, MATα, <i>Klbch1Δ::URA3</i>	This study
CRM2701	KHO69-8C, MATα, <i>Klchs6Δ::LEU2</i>	This study
CRM2712	KHO69-8C, MATα, <i>Klchs6Δ::LEU2 Klbch1Δ::URA3</i>	This study
<i>C. albicans</i>		
CAI4	<i>ura3::imm434/ura3::imm434</i>	Mio et al. (1996)
CRM693	CAI4, <i>chs3Δ::ura3Δ/chs3Δ::ura3Δ</i>	Sanz et al. (2005)
CRM743	CAI4, <i>chs3Δ/chs3Δ ura3Δ/ura3Δ</i>	Mio et al. (1996)
CRM2499	BWP17, (<i>ura3::imm434/ura3::imm434 his1::hisG/his1::hisG arg4::hisG/larg4::hisG</i>)	Enloe et al. (2000)
CRM2531	BWP17, <i>Cachs5Δ::ARG4/Cachs5Δ::HIS1</i>	This study
CRM2607	BWP17, <i>CHS3-GFP::SAT1</i>	This study
CRM2628	BWP17, <i>Cachs5Δ::ARG4/Cachs5Δ::HIS1 CHS3-GFP::SAT1</i>	This study
<i>U. maydis</i>		
CRM2442	FB1, <i>a1 b1</i>	Banuett and Herskowitz (1989)
CRM2443	FB1, <i>a1 b1, Umchs5Δ::hyg</i>	This study

to the chosen DNA locus. Specific protocols for this technique have been extensively described (Stuckey *et al.* 2011).

***K. lactis* constructions:** As in *S. cerevisiae*, gene deletions were made using the gene replacement technique; however, the DNA replacement cassette was highly concentrated (15×) (Rippert *et al.* 2017). In brief, cells (*his3:loxP ku80:loxP*, see Table 1) in log phase were made competent by resuspending them in a specific solution (1 M sorbitol, 1 mM bicine pH 8.35, and 3% ethylene glycol) and freezing the resuspension for at least 2 hr at -80° . Thawed cells were incubated for 5 min at 37° with 50 μ l of FISH DNA and ≈ 15 μ l of the target DNA. Then, a 40% polyethylene glycol 3300 solution was added and samples were incubated for 1 hr at 30° . Finally, the cells were washed and plated on selective growth media.

***C. albicans* constructions:** The replacement cassettes were made and concentrated in the same way as the *K. lactis* constructs. Yeast cells in log phase were transformed using a modified lithium acetate/electroporation protocol (Thompson *et al.* 1998).

***U. maydis* constructions:** Deletion mutants were generated using the *Golden Gate* procedure as described (Terfrüchte *et al.* 2014). In short, successive steps of cleavage, using the *Bsa*I restriction enzyme, and DNA ligation with T4 ligase generated a plasmid with the gene replacement module flanked by homologous regions 500 bp in length. For the transformation, protoplasts were generated using the Novozym extract and frozen at -80° . Thawed cells were incubated with heparin and concentrated DNA, incubated with 40% polyethylene glycol 4000, and finally plated on selective growth media as already described (Tsukuda *et al.* 1988).

Plasmid construction

The plasmids used throughout this work are described in Table 2.

Chs3 hybrid proteins (Sc-Ca) were constructed by homologous recombination *in vivo* in *S. cerevisiae* using centromeric plasmids and were expressed under the control of the native promoter of *ScCHS3*.

The Chs3 hybrid protein that contains the C-terminal end of CaChs3 (Chs3^{CaCT}-GFP) was constructed in two steps. First, the plasmid pHV7-GFP(*Not*I Δ) was linearized with *Not*I restriction enzyme and treated with Klenow fragment, and then cotransformed into wild-type *S. cerevisiae* together with the C-terminal fragment of *CaCHS3* (see Figure S6 in File S1), which had been previously amplified using dual primers designed from the genome of the *C. albicans* BWP17 strain. Several URA⁺ colonies were selected and the plasmids were rescued in *Escherichia coli* DH5 α . After construct verification by sequencing, a GFP tag was added to the end of the hybrid protein by homologous recombination in the *Scchs3* Δ mutant, using the appropriate cassette amplified from the pFA6a-GFP-*hphMx6* plasmid.

The N-terminal hybrid protein (CaNTChs3-GFP) was constructed using the plasmid pRS313-*CHS3*-GFP as a template.

The plasmid was linearized with *Age*I, treated with Klenow, and cotransformed into wild-type *S. cerevisiae* together with the N-terminal fragment of *CaCHS3* (see Figure S6 in File S1). HIS⁺ colonies were then selected, and their corresponding plasmids were rescued using *E. coli* DH5 α and sequenced.

Media and growth assays

Yeast cells were grown at 28° in YEPD (1% Bacto yeast extract, 2% peptone, and 2% glucose) or in synthetic (SD) medium (2% glucose and 0.7% Difco yeast nitrogen base without amino acids) supplemented with the pertinent amino acids, and 2% agar in the case of solid mediums. For the *C. albicans* strains, YEPD was supplemented with 80 mg-liter⁻¹ uridine (YEPDU). In most cases, NaCl was added to a final concentration of between 0.7 and 1 M, LiCl between 0.01 and 0.2 M, NH₄Cl between 0.1 and 0.2 M, hygromycin between 40 and 100 μ g·ml⁻¹, rapamycin between 2 and 20 nM, and calcofluor white (CW) between 0.01 and 0.1 mg·ml⁻¹. CW sensitivity was always tested on SD medium buffered with 50 mM potassium phthalate at pH 6.2 as described (Trilla *et al.* 1999). For some experiments, yeast extract, glucose, and supplements (YES) (0.5% Bacto yeast extract, 3% glucose, and 50 mg/liter each of adenine, L-histidine, L-leucine, L-lysine, and uracil) media was also used.

C. albicans filamentation was induced from stationary cultures as follows: cells from 200 μ l of a stationary culture, grown in YEPDU for at least 20 hr at 28° (OD₆₀₀ > 20), were recovered by centrifugation and resuspended in 5 ml of prewarmed filamentation media (YEPDU with 10% fetal bovine serum). This culture was incubated at 37° with agitation for 1–3 hr before the images were taken (Calderón-Noreña *et al.* 2015).

Drop tests

To assess the growth phenotypes, cells of each tested strain from fresh cultures were resuspended in water and adjusted to an OD₆₀₀ of 1.0. Ten-fold serial dilutions were prepared, and drops were spotted onto the appropriate agar plates containing media supplemented as indicated. Plates were incubated at 28° for 2–5 days.

Gradient plates were prepared by successively pouring two layers of media with different compositions. The first layer (containing the tested compound) was poured into a moderately inclined square Petri dish. After solidification, the plate was placed into a flat position and the second layer (with the same composition, only without the inhibitory compounds) was poured on top (Maresova and Sychrova 2005). In these experiments, the same diluted culture (OD₆₀₀ 0.1) was spotted along the plate.

Genetic screening

Wild-type yeast cells (BY4741, MATa *his3* Δ 1 *leu2* Δ 0 *met15* Δ 0 *ura3* Δ 0) were transformed using the LiAc method with 500 ng of a yEP52 genomic plasmid library (Carlson and Botstein 1982). Approximately 30,000 transformants were plated on YPD medium containing 75 μ g/ml CW. The colonies that grew on this media were retested for CW resistance

Table 2 Plasmids used

Plasmid	Genotype	Origin/reference
CRM264	pRS315	Laboratory collection
CRM264	pRS316	Laboratory collection
CRM254	pHV7::CHS3-GFP(NotIΔ)	Laboratory collection
CRM1131	pRS315::CHS3-GFP	Sacristan <i>et al.</i> (2013)
CRM1253	pRS313::CHS3-GFP	Sacristan <i>et al.</i> (2013)
CRM1929	pRCW3 (yEP52::BCH2::LEU2)	This study
CRM1934	pJV30 (PTPI-BCH2::LEU2)	This study
CRM1205	pRS316::FUS1-GFP	Santos and Snyder (2003)
CRM2670	pHV7::CHS3 ^{CaCT} -GFP::hphNT1	This study
CRM2650	pRS313::CaNTCHS3-GFP	This study
CRM2546	pAG25 (<i>natMx4</i>)	Goldstein and McCusker (1999)
CRM1188	pUG6 (<i>kanMx4</i>)	Goldstein and McCusker (1999)
CRM1451	pFA6a- <i>hphNT1</i>	Goldstein and McCusker (1999)
CRM2037	pFA6a- <i>kanMx6</i> -PGAL1	Longtine <i>et al.</i> (1998)
CRM1995	pFA6a-GFP- <i>hphNT1</i>	Sato <i>et al.</i> (2005)
CRM1811	pFA6a-GFP- <i>natMx4</i>	Sato <i>et al.</i> (2005)
CRM2653	pFN21 (<i>mCherry-natMx4</i>)	Sato <i>et al.</i> (2005)
CRM2360	pGSHU (CORE Delitto Perfetto)	Stuckey <i>et al.</i> (2011)
CRM2620	pJH955L (<i>LEU2</i>)	Heinisch <i>et al.</i> (2010)
CRM2621	pJH955U (<i>URA3</i>)	Heinisch <i>et al.</i> (2010)
CRM3236	pFA-CaHIS1	Gola <i>et al.</i> (2003)
CRM3238	pFA-CaARG4	Gola <i>et al.</i> (2003)
CRM2583	pFA-GFP-SAT1	Schaub <i>et al.</i> (2006)

and later expanded, and the plasmids were isolated and sequenced.

Fluorescence microscopy

Yeast cells expressing GFP/mCherry-tagged proteins were grown to early logarithmic phase in SD medium supplemented with 0.2% adenine. Living cells were visualized directly by fluorescence microscopy. Filamentation of *C. albicans* was performed on YEPDU media, where the cells were washed once with SD medium before being visualized.

CW staining

Two different protocols were used throughout the work as described (Arcones and Roncero 2016). For vital staining, CW was directly added to 50 $\mu\text{g}\cdot\text{ml}^{-1}$ of the fresh cells growing on rich media, and then cultures were incubated at 28° for 1 hr. For staining of fixed cells, 1 ml of logarithmic culture was centrifuged, and cells were resuspended in 200 μl of 3.2% formaldehyde and incubated at 4° for 30 min. Then, aliquots were washed twice with PBS and incubated for 5 min with 50 $\mu\text{g}\cdot\text{ml}^{-1}$ CW. For hyphal staining, fixed filaments were previously separated by incubation with proteinase K at 34° for 30 min and later stained as indicated.

Microscopic images were obtained using a Nikon 90i epifluorescence microscope ($\times 100$ objective; NA: 1.45) (Nikon, Garden City, NY), equipped with a Hamamatsu ORCA ER digital camera. Tagged proteins were visualized using a 49002 ET-GFP (FITC/Cy2) filter for GFP and a 49005 ET-DsRed (TRITC/Cy3) filter for mCherry. A 49000 ET-DAPI filter was used for CW staining (Chroma Technology). The images were then processed using ImageJ software (National Institutes of Health) and mounted with Adobe Photoshop

CS5 (San José, CA) software. All images shown in each series were acquired under identical conditions and processed in parallel to preserve the relative intensities of fluorescence for comparative purposes. In all figures, the white bar represents 5 μm .

When necessary, image measurements obtained with ImageJ were statistically analyzed using the Student's *t*-test for unpaired data. Analyses were performed using GraphPad Prism (GraphPad Software, Inc., La Jolla, CA) software. Significantly different values ($P < 0.05$, $P < 0.01$, and $P < 0.001$) are indicated (*, **, and ***).

Protein extracts and immunoblotting

Total cell lysates were prepared by resuspending cells from 30 ml logarithmic phase cultures in 150 μl of lysis buffer (50 mM Tris-HCl pH 8, 0.1% Triton, and 150 mM NaCl) containing 1 \times protease inhibitor cocktail (1 mM PMSF, 1 $\mu\text{g}\cdot\text{ml}^{-1}$ aprotinin, 1 $\mu\text{g}\cdot\text{ml}^{-1}$ leupeptin, and pepstatin A 1 $\mu\text{g}\cdot\text{ml}^{-1}$). Cells were disrupted using glass beads (0.45 mm; Sigma [Sigma Chemical], St. Louis, MO) during three pulses of 15 sec each with an intensity of 5.5 units in a Fast prep cell disrupter (FP120, BIO101). Cell debris was eliminated by centrifugation (5 min, 10,000 $\times g$ at 4°) and the resultant supernatant was boiled for 5 min with 4 \times sample buffer (0.2 M Tris-HCl pH 6.8, 4% SDS, 40% glycerol, and 4% β -mercaptoethanol). Next, 100 μg of protein per sample were separated by 7.5% SDS-PAGE and transferred to PVDF membranes (Trilla *et al.* 1999). The membranes were then blocked with skimmed milk and incubated with the corresponding antibodies: anti-GFP JL-8 monoclonal antibody (Living colors, Clontech) and anti-tubulin (T5162; Sigma). Blots were developed using an ECL kit (Advansta).

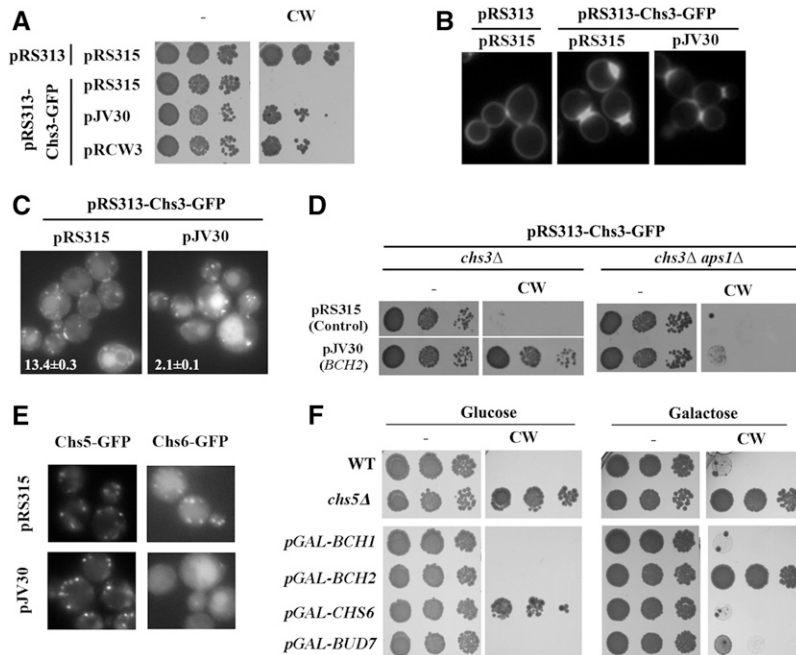


Figure 1 Phenotypes of *BCH2* overexpression. (A) Calcofluor white (CW) resistance promoted by multicopy plasmids pRCW3 and pJV30, both containing *BCH2*. (B) CW vital staining of the indicated strains. Note the reduction of fluorescence after *BCH2* overexpression. (C) Localization of Chs3-GFP in *chs3Δ* strains transformed with the indicated plasmids. Numbers indicate the percentage of cells showing localization at the neck ($n > 100$). (D) CW resistance of the indicated mutants transformed with control or pJV30 plasmids. Note the sensitization to CW in the *aps1Δ* mutant after *BCH2* overexpression. These experiments were always performed in strain CRM1590 (*chs3Δ::natMx4*) transformed with plasmids pRS315 or pRS315-Chs3-GFP as indicated. (E) Localization of Chs5-mCh and Chs6-mCh after *BCH2* overexpression (pJV30). Chs5-mCh and Chs6-mCh are tagged on the chromosome. (F) CW resistance after overexpression of the different ChAPs. Experiment was carried out in wild-type (WT) cells in which the *pGAL* promoter was inserted at the chromosome replacing the endogenous promoter of each ChAP. Overexpression of the different ChAPs was achieved by growth in galactose-supplemented media. Note that cells grown in glucose should behave similarly to null mutants of the corresponding genes. Also see Figure S2 in File S1 for a more complete set of experiments.

Data availability

All the strains and plasmids used throughout the work are described in Table 1 and Table 2, and are available upon request.

Results

Bch2 is a ChAP with distinct characteristics

Chs3 depends on complex molecular machinery for its delivery to the PM (Roncero 2002). In addition, Chs3 has been shown to contain several post-translational modifications that affect its intracellular transport. These include palmitoylation (Lam *et al.* 2006), N-glycosylation (Sacristan *et al.* 2013), and ubiquitination (Arcones *et al.* 2016). Therefore, we aimed to identify yeast proteins that, when overproduced, would alter the intracellular transport of Chs3 leading to CW resistance due to the reduction of Chs3 levels at the PM. Consequently, we performed a screen for yeast genes that, when overexpressed in the yEP52 plasmid, would confer CW resistance. Among the plasmids isolated in this screen, the plasmid RCW3 contained the *BCH2* gene previously linked to the function of Chs3 (Trautwein *et al.* 2006) and was used to carry out the work presented here.

BCH2 was subcloned into plasmid pJV30 under the control of the strong triose phosphate isomerase (*TPI*) promoter, a construct that also promoted CW resistance (Figure 1A). Moreover, overexpression of *BCH2* using the plasmid pJV30 resulted in a strong reduction in fluorescence after CW staining (Figure 1B), consistent with a reduction in chitin synthesis in these cells. This result was compatible with our original hypothesis that the overexpression of some proteins could affect Chs3 trafficking; therefore, the intracellular localization of Chs3-GFP after *BCH2* overexpression was addressed. It was found that Chs3-GFP was mostly localized at intracellular

spots resembling the TGN in cells containing the pJV30 plasmid (Figure 1C). Moreover, localization of Chs3-GFP at the neck was severely impaired, which explained resistance to CW and the lower fluorescence staining observed in these strains. The absence of Chs3 at the ER after *BCH2* overexpression discounted the idea of any role of Bch2 in the exit of Chs3 from the ER, suggesting that Chs3 might be retained at the TGN. Interestingly, Bch2 is a member of the exomer, a complex that is involved in the exit of Chs3 from the TGN (Trautwein *et al.* 2006). In the absence of a functional exomer, its cargos are retained in the TGN and their delivery to the PM is rescued by deletion of the clathrin adaptor complex AP-1; therefore, the effects of *BCH2* overexpression in the *aps1Δ* mutant were addressed. As shown in Figure 1D, deletion of AP-1 alleviated the effects of *BCH2* overexpression, restoring CW sensitivity. Together, these results are consistent with a defect in exomer function with respect to Chs3 traffic after *BCH2* overexpression. To test whether this defect was due to a general failure of exomer assembly or one that specifically affected Chs3 transport, the localization of Chs5 and Chs6 proteins was monitored. The dotted Chs5 localization was not affected by pJV30, but Chs6, the ChAP protein acting as the dedicated cargo adaptor for Chs3, was not assembled into the exomer, as can be seen by its diffuse cytoplasmic localization upon *BCH2* overexpression. Moreover, the high level of Bch2 did not affect the intracellular localization of the other exomer cargos Fus1 and Pin2 (see Figure S2 in File S1 and Table 3). Apparently, high levels of Bch2 specifically displaced the dedicated cargo adaptor for Chs3 from the exomer complex.

Then, we addressed whether overexpression of other ChAPs would have similar effects by expressing individual ChAPs from the strong inducible *GAL1* promoter. In glucose media, only the absence of *CHS6* led to CW resistance, the

same result as reported for the *chs6Δ* mutant (Trautwein *et al.* 2006). In galactose, overexpression of *BCH2*, but not of any of the other ChAPs, promoted CW resistance (Figure 1F). In addition, none of the overexpressed ChAPs produced sensitivity to lithium, another classical phenotype associated with the absence of exomer (Ritz *et al.* 2014) (see Figure S2 in File S1 and Table 3). However, overexpression of *BCH2* also caused partial sensitivity to ammonium that may be associated with the reduced functioning of the Bud7/Bch1 proteins.

Altogether, these results indicate that the deleterious effects of ChAPs overexpression are specific for *BCH2* and directly linked to *Chs6* function, probably due to the similarity between these proteins (Trautwein *et al.* 2006). Interestingly, *Bch2* contains a unique C-terminal region (see Figure S3A in File S1) that makes it longer than any of the other ChAPs. This region includes a potential SH3 interaction domain (Tonikian *et al.* 2009). To assess the potential function of the C-terminal region, the most C-terminal 31 amino acids were deleted. Wild-type *Bch2*-GFP typically localizes at the TGN but, after overexpression, *Bch2*-GFP also appeared extensively associated with cellular membranes (Figure S3, B and C in File S1). However, while *Bch2*^{Δ31}-GFP localized at the TGN, similar to the wild-type protein, its overexpression did not lead to it being accumulated on internal membranes to the same extent (Figure S3, B and C in File S1). The primary TGN localization signal appeared to be upstream of the unique C-terminal region, because a larger deletion in the C-terminal region of *Bch2* (Δ118) completely altered the TGN localization of the protein. More importantly, unlike overexpression of *Bch2*-GFP, overexpression of *Bch2*^{Δ31}-GFP did not produce CW resistance, indicating that the effects of *BCH2* overexpression on *Chs3* transport are associated with its unique C-terminal region (Figure S3D in File S1). However, this region is not the only reason for the CW resistance phenotype, as transplanting the C-terminal region of *Bch2* onto *Bch1* did not promote CW resistance upon overexpression (Figure S3E in File S1).

The evolutionary story of the ChAPs family

Our results clearly indicated that *Bch2* behaved differently from other members of the ChAPs family. Therefore, we addressed the evolutionary divergence among the different ChAPs, taking into consideration that exomer is a complex that is conserved across the fungi kingdom. While the exomer scaffold *Chs5* is well conserved across fungi (Roncero *et al.* 2016), the ChAPs are not, since most fungi contain a unique ChAP. Moreover, duplication of ChAPs occurred later on in their evolution because more than one ChAPs can only be found within the Saccharomycotina group (Figure 2A, see also Figure S4 in File S1). A direct comparison of ChAPs sequences (Figure 2B) indicated that the oldest ChAP, *Bch1*, was relatively well conserved, and the dendrogram identified three separated clades that resembled the evolutionary history of the Saccharomycotina group. When *Bch1* sequences from different fungi (Figure 2B) were compared, early branching

Table 3 Effects of altering exomer configuration by deleting or overexpressing different ChAPs

Strain	Growth ^a					Cargo localization ^b		
	CW	LiCl	NaCl	Hyg	NH ₄ Cl	Chs3	Fus1	Pin2
WT	—	++	++	++	++	+	+	+
<i>chs5Δ</i>	+++	—	—	—	—	—	—	—
<i>chs6Δ</i>	+++	++	++ ^c	NT	++	—	+	+
<i>bch2Δ</i>	—	++	++ ^c	NT	++	+	+	+
<i>bch1Δ</i>	—	++	NT	NT	++	+	+	+
<i>bud7Δ</i>	—	++	NT	NT	++	+	+	+
<i>chs6Δ bch2Δ</i>	+++	—	+	++	++	—	—	+
<i>bch1Δ bud7Δ</i>	+++	++	+	—	±	—	—	+
<i>pGAL-BCH1^{OE}</i>	—	++	++	++	++	+	+	+
<i>pGAL-BCH2^{OE}</i>	+++	++	++	++	+	—	+	+
<i>pGAL-BUD7^{OE}</i>	—	++	++	++	++	+	+	±
<i>pGAL-CHS6^{OE}</i>	—	++	++	++	++	+	+	+

WT, wild-type; NT, not tested.

^a Growth was assessed on YEP plates, using glucose or galactose (OE) as carbon sources and defined as being from maximum (++++) to minimum (—). Also see Figure S2 in File S1 for the real results after serial dilutions of the different strains.

^b Localization was assessed microscopically using the tagged versions of the exomer cargos Chs3-GFP, Fus1-GFP, and Pin2-GFP expressed from their own promoters from centromeric plasmids or the chromosome, as indicated in *Materials and Methods*. (+) indicates normal arrival of the cargo at the PM, while (—) indicates retention at the *trans*-Golgi network.

^c Data collected from previous reports (Trautwein *et al.* 2006; Ritz *et al.* 2014).

genera, such as *Yarrowia*, (Figure 2, A and B) appeared preferentially associated with fungi from the other major groups rather than with other members from the Saccharomycotina. This *Bch1* comparison clearly separated the CTG clade (species that translate CTG codon as serine) (Wang *et al.* 2009) within the Saccharomycotina group. Both CTG and non-CTG-containing genera contained two ChAPs, but the direct comparison of the second ChAP, *Chs6*, clearly differentiated the two. Also, the CTG members that were outside the main branches of the tree had very divergent versions of *Chs6* (Figure 2B), with some intermediate representatives like *Wickerhamomyces anomalus*. Somehow these differences effectively recapitulate the evolutionary history reported within the Saccharomycotina group (Figure 2A). Later on, the whole-genome duplication (WGD) associated with the WGD clade (*Saccharomyces* genus) led to the appearance of the four ChAPs that have been previously identified and characterized in *S. cerevisiae*.

Addressing exomer function across fungi

Considering the evolutionary divergence of the ChAPs family, additional studies were conducted to investigate the most primitive function of exomer by deleting *CHS5*, the core component of exomer in several fungi. The basidiomycete *U. maydis* and the CTG representative *C. albicans* were chosen because chitin synthesis has been studied in some detail in both organisms (Weber *et al.* 2006; Lenardon *et al.* 2010b). In addition, *K. lactis* was used as a close relative of *S. cerevisiae* without genome duplication. Deletions were performed as described for each organism (see *Materials and Methods* section for details), and CW resistance was addressed using the corresponding *chs3Δ* mutant as a control. As shown in Figure 3A, deletion of *CHS5* only conferred resistance to CW

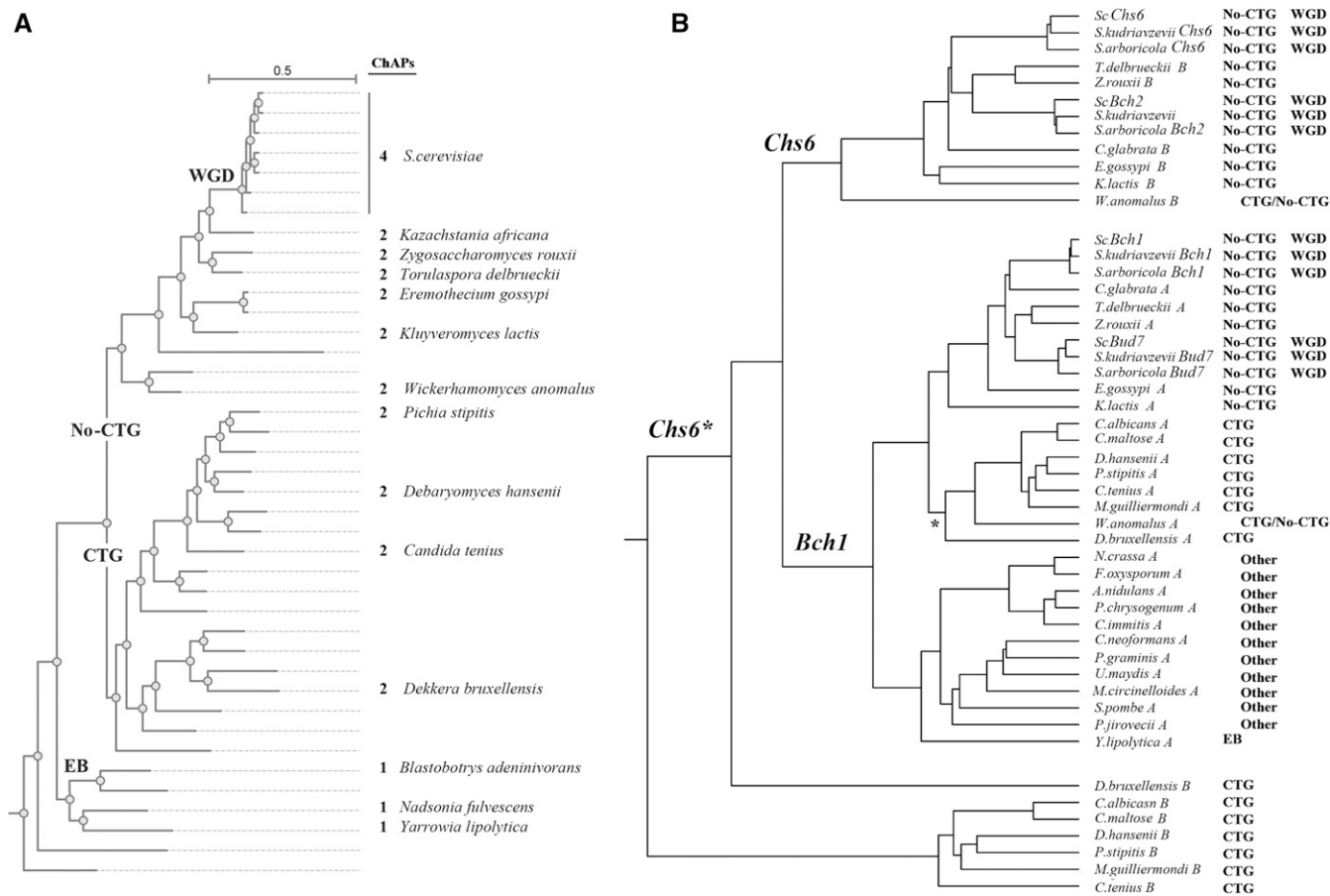


Figure 2 Phylogeny of ChAPs (Chs5-Arf1 binding proteins) along fungi. (A) Phylogenetic tree of the Saccharomycotina clade. Major evolutionary lineages are indicated, including the proposed EB groups. Tree images were obtained from MycoCosm portal (Grigoriev *et al.* 2014). The number of ChAPs members identified in each group is indicated on the right. Note the presence of a single ChAP in all early branched genera, which is similar to other major groups of fungi (see also Figure S4 in File S1). (B) A phylogenetic analysis of the ChAPs family. Individual proteins were identified by BLAST analysis and a multiple alignment with CLUSTALW was later performed. Analysis is represented as a rooted phylogenetic tree (UPGMA) with branch lengths. Only the genes within the genus *Saccharomyces* have been named, and the letters A and B have been used to indicate the homologous closest to *ScBch1* and *ScChs6*, respectively. See text for a more detailed description of the tree. BLAST, basic local alignment search tool; CTG, species that translate CTG codon as serine; EB, early branched; WGD, whole-genome duplication.

in *S. cerevisiae*. This result is consistent with the absence of caspofungin sensitivity outside *S. cerevisiae* considering that both phenotypes have been previously linked to defective chitin synthesis (Markovich *et al.* 2004). Next, chitin was visualized directly using CW staining after cell fixation (Figure 3B). Chitin rings similar to those of wild-type were neatly visible in *Klchs5Δ* and *Cachs5Δ* strains at the neck region, but not in the corresponding *chs3Δ* controls. Likewise, *U. maydis chs5Δ* cells also showed apparent normal CW staining. Surprisingly, the best-studied role of exomer in *S. cerevisiae*, namely controlling *Chs3* PM localization and hence chitin synthesis, is not conserved in *U. maydis*, *C. albicans*, or even *K. lactis*.

S. cerevisiae exomer mutants display additional phenotypes like sensitivity to cationic compounds or rapamycin (Parsons *et al.* 2004). Therefore, these exomer mutant phenotypes were also tested in these other fungi (Figure 3C). As a result, no phenotypes were found for *U. maydis* or *C. albicans chs5Δ* mutants, except for a slight sensitivity to rapamycin. However, the *K. lactis chs5Δ* mutant was sensitive to lithium and

hygromycin, the same as *S. cerevisiae* (see also Figure 4A). However, in contrast to *Scchs5Δ*, *Klchs5Δ* was resistant to high concentrations of NaCl.

In summary, most of the phenotypes associated with the absence of exomer in *S. cerevisiae*, including reduced chitin synthesis or sensitivity to NaCl, were not observed in other fungi, and only sensitivity to LiCl was observed in *K. lactis*, a close relative of *S. cerevisiae*. Taken together, our data indicate that at least some of the exomer functions reported to date were most probably acquired in correlation with the expansion of the ChAPs family.

ChAPs have maintained redundant functions in *K. lactis*, but have acquired divergent functions in *S. cerevisiae*

If the previous statement is true, then what is the conserved function of exomer? To answer this question, the phenotypes exhibited by the different exomer mutants of *K. lactis* and *S. cerevisiae* were studied. In *S. cerevisiae*, individual ChAPs mutants other than *chs6Δ* had no clear phenotypes (Table 3),

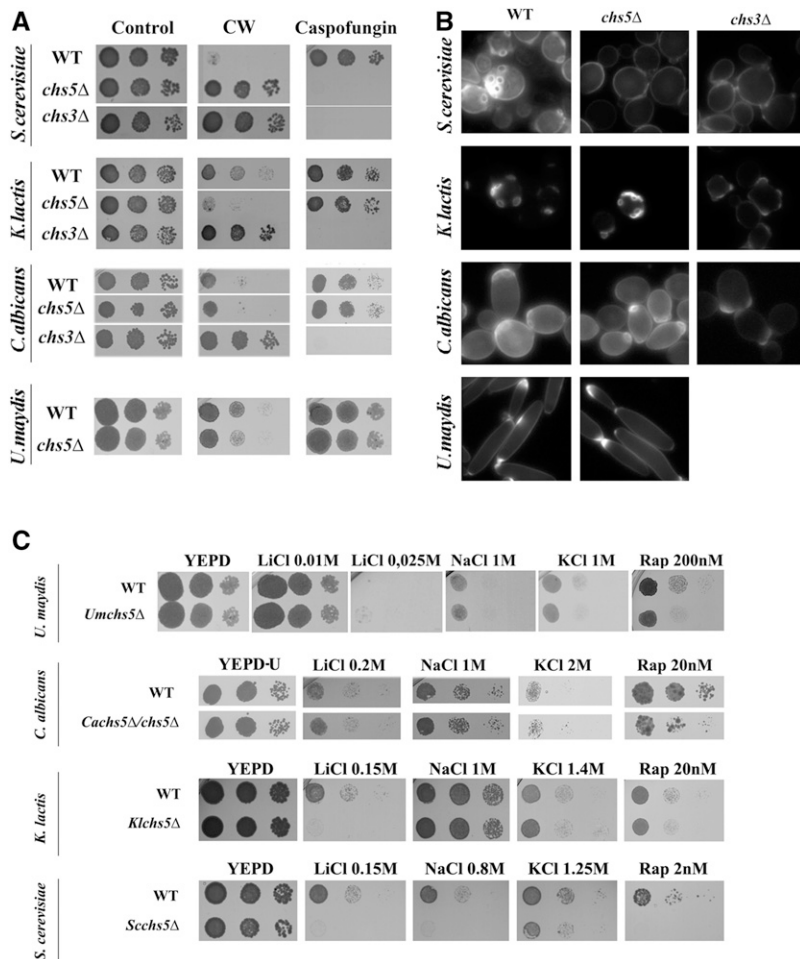


Figure 3 Characterization of exomer mutants in different fungi. (A) Sensitivity of the *chs5Δ* mutants of different fungi to calcofluor white (CW) and caspofungin, as compared to the corresponding wild-type (WT) and *chs3Δ* mutants used as controls. *chs3Δ* mutants were resistant to CW and sensitive to caspofungin in all organisms, but only the *S. cerevisiae chs5Δ* exomer mutant reproduced this phenotype. (B) CW staining of fixed cells on the indicated strains and organisms. Note the absence of chitin rings in all the *chs3Δ* mutants, which did not occur in the *chs5Δ* mutant, except in *S. cerevisiae*. *U. maydis chs5Δ* mutant showed normal CW vital staining. (C) Extended characterization of phenotypes of the different mutants. Cells were grown to early logarithmic phase, serially diluted, and plated on the indicated media. Growth was scored after 2–3 days of growth at 28°.

owing to genetic redundancy between the homologous protein pairs *Bud7/Bch1* and *Chs6/Bch2*. Only the simultaneous deletion of both *CHS6* and *BCH2* genes produced lithium sensitivity in *S. cerevisiae*, which turned out to be identical to that of the *chs5Δ* mutant (Figure 4A). In contrast, the *bch1Δ bud7Δ* double mutant was sensitive to hygromycin like the *chs5Δ* mutant, but the mutant *chs6Δ bch2Δ* was not (Figure 4A). All together, these results indicate that the *S. cerevisiae* ChAPs pairs have distinct and nonredundant roles regarding their function on exomer. In *K. lactis*, the individual ChAPs mutants exhibited no distinctive phenotypes, since both *Klbch1Δ* and *Klchs6Δ* mutants were resistant to lithium and hygromycin, similar to wild-type (Figure 4B). Furthermore, only deletion of both ChAPs (*Klbch1Δ chs6Δ* mutant) fully reproduced the phenotypes associated with the absence of exomer (*Klchs5Δ*), a clear indication of the functional redundancy between both ChAPs.

Next, the sensitivity of *S. cerevisiae* exomer mutants to a high concentration of NH_4^+ in both defined (not shown) and rich media (Figure 4C, see also Figure S2 in File S1) was analyzed. This sensitivity could be distinctively linked to the function of *Bch1/Bud7*, since the *chs6Δ bch2Δ* mutant grew in a similar way as the control. The *K. lactis chs5Δ* mutant was not sensitive to a high concentration of ammonium; however, the mutant

showed reduced growth on YES media (Figure 4C). YES is a complex media capable of supporting the growth of *S. cerevisiae* using yeast extract and a limited supply of amino acids (histidine, leucine, and lysine; see *Materials and Methods* for further details on the media composition) as the nitrogen source. Figure 4C shows that *Klchs5Δ*, as well as *Klbch1Δ* and *Klchs6Δ*, were not able to grow on YES media, but that NH_4^+ restored the full growth of all of these strains. Moreover, amino acids like Asp or Glu, which are used as the preferred nitrogen source in yeast, also improved the growth of the *Klbch1Δ* ChAP mutant, although this was not the case of the *Klchs5Δ* mutant lacking a functional exomer. Other amino acids did not have an effect on the growth of any of the strains tested. Interestingly, the *Klchs6Δ* mutant grew normally on YES media but, in the absence of *Bch1*, the presence of a functional *Chs6* was required for the use of Asp or Glu as a nitrogen source, since these amino acids were not able to improve the growth of the double *Klbch1Δ chs6Δ* mutant. These results indicate that the *K. lactis* exomer mutants have a significant defect in the utilization of amino acids as a source of nitrogen, which requires the presence of at least one functional ChAP. This result reinforces the idea that both ChAPs are functionally redundant in this organism, although the role of *Bch1* in this process seems to be more important.

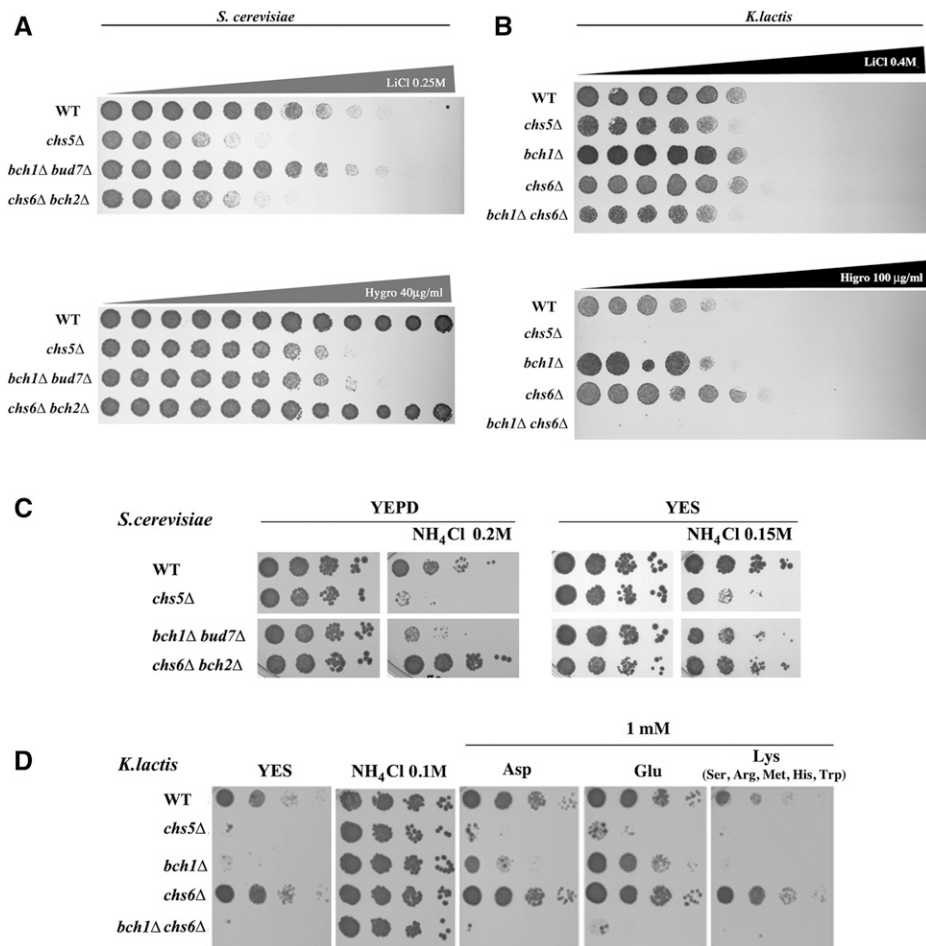


Figure 4 Phenotypic characterization of exomer mutants in *S. cerevisiae* and *K. lactis*. Growth of the indicated *S. cerevisiae* (A) and *K. lactis* (B) mutants on YEPD gradient plates containing increasing concentrations of different compounds. Logarithmic cultures were diluted OD₆₀₀ 0.1 and spotted at identical concentrations along the gradient plate. (C) Growth of the indicated *S. cerevisiae* strains on complex media supplemented with NH₄Cl. (D) Growth of the indicated *K. lactis* mutants on YES media supplemented with the indicated nitrogen sources. Panel on the right represents the plate supplemented with Lys, where the results with either amino acid were identical. (C and D) show early logarithmic phase cultures grown on YEPD that were serially diluted and spotted onto the different plates. Note the specific sensitivity of *S. cerevisiae* exomer mutants to high concentrations of NH₄Cl, which is not observed in the corresponding mutant in *K. lactis*. The individual ChAPs mutants of *S. cerevisiae* did not show sensitivity toward any of the compounds used in this figure (see Figure S2B in File S1), therefore only the double ChAPs mutants were tested. *K. lactis* contains only two ChAPs, therefore the results for the individual mutants are presented. Note that in *S. cerevisiae* always one of the double mutants behaved exactly as the null exomer mutant *chs5Δ*, while in *K. lactis* the individual mutants lacked phenotype and only the absence of the two ChAPs showed a phenotype equivalent to the null *chs5Δ* mutant. YEPD, 1% Bacto yeast extract, 2% peptone, and 2% glucose; YES, yeast extract, glucose, and supplements; WT, wild-type.

Exomer regulates chitin synthesis localization in *C. albicans*

Chitin synthesis in *C. albicans* is well documented and is mainly dependent on the delivery of CaChs3 to the PM (Sanz *et al.* 2005; Lenardon *et al.* 2010a). Previously, it was said that the amount of chitin seemed similar in the *chs5Δ* and wild-type strains of *C. albicans* after CW staining and, accordingly, the *Cachs5Δ* mutants did not show significant changes in their sensitivity to CW or caspofungin (Figure 3). However, upon CW vital staining, it was observed that fluorescence was partially delocalized in the *C. albicans chs5Δ* mutant, which showed lateral staining in most buds in addition to the normal staining at the neck (Figure 5A). Moreover, in the wild-type strains, chitin was uniformly distributed during hyphal elongation except at the tip of the hypha. This distribution was similar to that observed in the *chs5Δ* mutant, although a longer portion of the tip remained consistently devoid of fluorescence in the mutant (Figure 5A, see also Figure S5 in File S1), suggesting a partial delocalization of chitin. This defect did not significantly affect *C. albicans* morphogenesis since cell filamentation occurred normally in the exomer mutants under all the conditions tested (Figure S5 in File S1 and data not shown). To understand this

phenotype, CaChs3 localization was determined by tagging the endogenous *CaCHS3* gene with GFP (Sacristan *et al.* 2012). In the wild-type strain, CaChs3-GFP appeared mostly localized at the neck of yeast cells and also showed a partial distribution along the membrane of the small buds (Figure 5, B and C). The *Cachs5Δ* mutant showed a similar accumulation of CaChs3-GFP at the neck, but fluorescence seemed to be strongly reduced in the bud membranes (Figure 5, B and C). Moreover, the intracellular spots observed for Chs3 were significantly more intense than in the wild-type. Similar results were observed during hyphal growth, where CaChs3 was fully polarized in the tips of wild-type cells with a neat gradient extending from the tip. This polarization seemed reduced in the *Cachs5Δ* mutant, showing a more uniform distribution of the protein along the tip (Figure 5B and Figure S5B in File S1), which was associated with a higher accumulation of the protein at intracellular spots. Altogether, these results indicate that CaChs3 efficiently reaches the PM in the absence of exomer. However, exomer could have a role in the polarized delivery of CaChs3 from the TGN, a finding that is similar to what has been recently observed for the *Ena1* protein of *S. cerevisiae* (Anton *et al.* 2017).

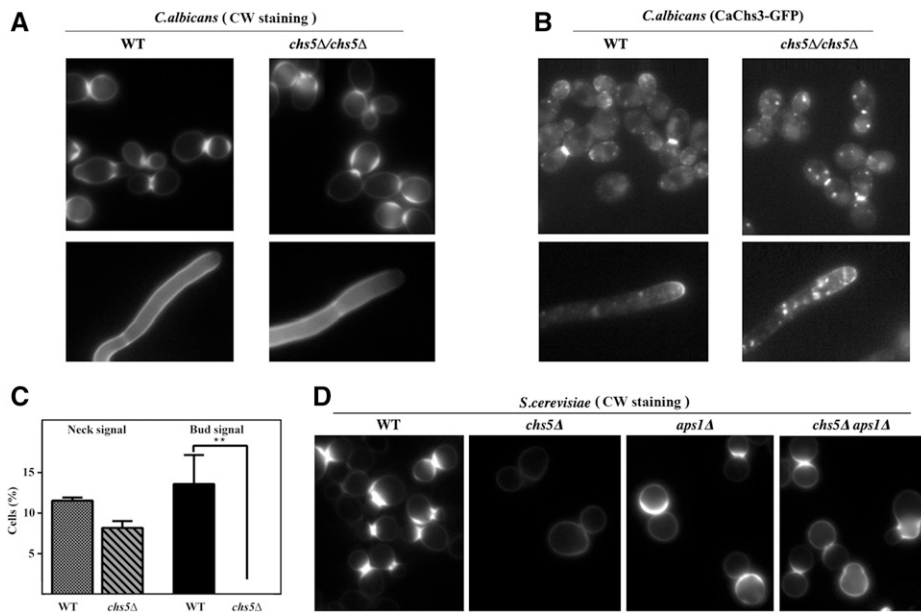


Figure 5 Characterization of chitin synthesis in *C. albicans*. (A) CW vital staining of *C. albicans* yeast cells strains as indicated (upper panels). Staining was performed for 60 min. For hyphal visualization (lower panels), filamentation was induced for 2 hr and staining was performed on fixed cells as described in the *Materials and Methods* section. Note the different localization of chitin in the mutant in both yeast and hyphal cells. (B) Intracellular localization of CaChs3-GFP on yeast and hyphal cultures. (C) Panel represents numerical analysis of CaChs3-GFP localization in yeast ($n = 3$, >100 cells counted in each experiment). Note the apparent loss of signal for CaChs3-GFP in the buds of the exomer mutant. (D) CW vital staining of the indicated mutants of *S. cerevisiae*. Note the partial delocalization of chitin to the bud in the *aps1Δ* mutants, a result similar to that observed in the *Cach5Δ* mutant (A). See Figure S5 in File S1 for additional data on chitin and CaChs3-GFP localization. CW, calcofluor white; WT, wild-type.

A similar situation has been previously described in *S. cerevisiae*, where the absence of the AP-1 complex resulted in partially delocalized chitin deposition (Figure 5D). Moreover, a double mutant (*chs5Δ aps1Δ*) lacking exomer and AP-1 complexes regained chitin synthesis and CW sensitivity as compared to the single exomer mutant (*chs5Δ*) (Figure 5D) (Valdivia *et al.* 2002). However, chitin localization in this double mutant was more diffuse than in the wild-type (Figure 5D), being also partially resistant to CW. This behavior has been linked to the interaction of ScChs3 to both exomer and AP-1 complexes through specific cytosolic domains of the protein (Rockenbauch *et al.* 2012; Starr *et al.* 2012). Thus, a simple explanation for the results found in *C. albicans* may be associated with the different interactions of CaChs3 with these complexes.

However, whether or not the differences between the ScChs3 and CaChs3 proteins are enough to sustain such a hypothesis still needs to be addressed. It is known that both proteins have a very similar sequence (see Figure S6 in File S1) with >50% overall identity and 61% identity in the region containing the catalytic domain of the protein. However, the C-terminal region of CaChs3 is significantly longer. Interestingly, this lengthy C-terminal cytosolic region is also present in the Chs3 of different fungi (Figure S6B in File S1), indicating unique properties for the Chs3 from *Saccharomyces*, even between the non-CTG clade. Moreover, the N-terminal region of both proteins is also divergent and, more importantly, the first 50 amino acids are very different (Figure S6C in File S1). These N- and C-terminal regions of ScChs3 contain the domains required for its interaction with AP-1 and exomer complexes. Therefore, it is tempting to speculate that the differences in these regions between ScChs3 and CaChs3 (see Figure S6, C and D in File S1) are responsible for the different behavior. This question was addressed by

investigating the behavior of chimeric Chs3 proteins in *S. cerevisiae*. CaChs3 has been shown to be nonfunctional in *S. cerevisiae* because of its extensive retention at the ER (Jimenez *et al.* 2010). Thus, hybrid proteins were generated by replacing the N- and C-terminal regions of ScChs3 with their corresponding regions from CaChs3. The protein Chs3^{CaCT}, which contains the C-terminal region of CaChs3 (see Figure S6D in File S1 for details on the construction), was not functional since cells expressing this chimaera were resistant to CW (Figure 6A) and showed reduced levels of chitin after CW staining (Figure 6B). In contrast, the protein Chs3^{CaNT}, which contains the N-terminal region (see Figure S6C in File S1 for details), was functional because its expression led to normal chitin levels. When these proteins were expressed in the *Scchs5Δ* mutant, the Chs3^{CaCT}-containing strains had no chitin and were resistant to CW. This was also the case for the strain expressing wild-type ScChs3. However, the Chs3^{CaNT} protein promoted chitin synthesis as shown by CW staining and sensitivity to this drug (Figure 6, A and B), a phenotype very similar to that observed after the expression of the L^{24A}ScChs3 protein (Starr *et al.* 2012). When expressed in the *aps1Δ* mutant, the Chs3^{CaCT} sustained partial chitin synthesis conferring CW sensitivity, while Chs3^{CaNT} behaved similar to the wild-type ScChs3. In agreement with these phenotypic results, Chs3^{CaCT}-GFP was unable to efficiently reach the neck region in the wild-type strain, although deletion of *APS1* restored the arrival of this chimeric protein at the PM (Figure 6, C and D). Moreover, Chs3^{CaNT}-GFP partially reached the PM, even in the absence of exomer (Figure 6, C and D). Therefore, our results indicate that the N- and C-terminal regions of CaChs3 are unable to efficiently mediate the interaction of these hybrid proteins with AP-1 and exomer, respectively, although it could be argued that these results were obtained with chimeric proteins in a heterologous host such as *S. cerevisiae*. However, the

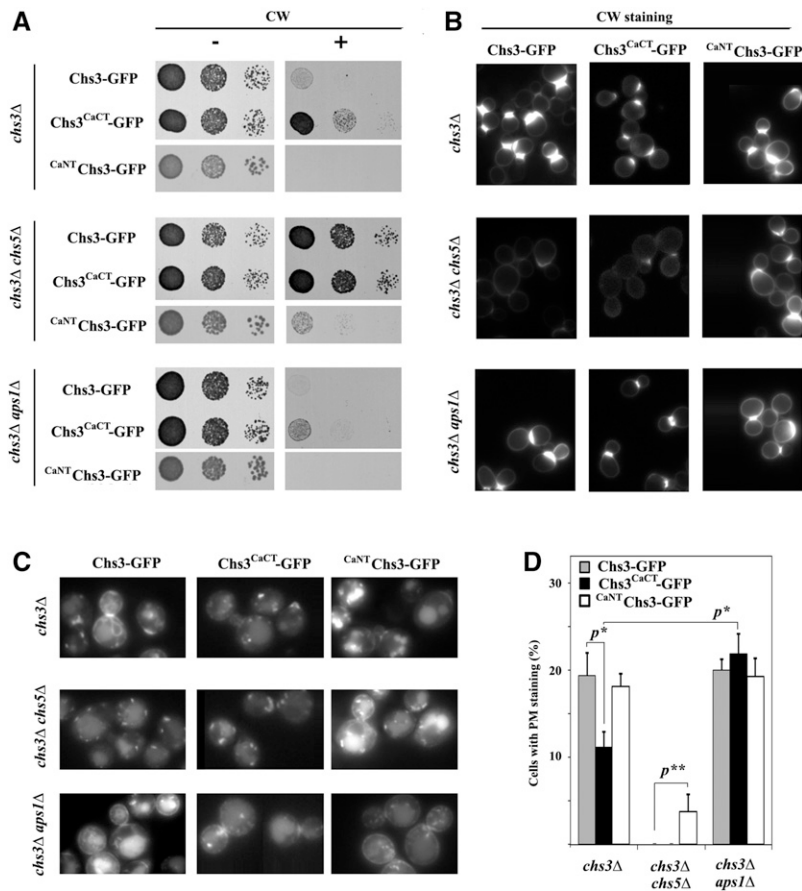


Figure 6 Functional characterization of chimeric Chs3 proteins. (A) Calcofluor (CW) resistance promoted by the chimeric proteins Chs3^{CaCT}-GFP and CaNT Chs3-GFP in the indicated *S. cerevisiae* strains compared to the wild-type ScChs3-GFP used as the control. (B) CW vital staining of the same strains as in (A). (C) Intracellular localization of ScChs3-GFP, Chs3^{CaCT}-GFP, and CaNT Chs3-GFP in the indicated strains. (D) Quantitative analysis of the images in (C) ($n = 4$, >100 cells/experiment). Note the reduced arrival of Chs3^{CaCT}-GFP at the PM, which is restored in the *aps1Δ* mutant. In contrast, CaNT Chs3-GFP arrives partially at the PM even in the *chs5Δ* mutant. See Figure S6 in File S1 and *Materials and Methods* for details on the chimeric constructs.

in vivo results obtained for *C. albicans* (Figure 4 and Figure 5) strongly support the model in which CaChs3 does not depend on exomer for Chs3 delivery to the PM, justifying the absence of exomer- and AP-1-interacting domains in this protein. Apparently, the physiological dependence on exomer and AP-1 for the trafficking of Chs3 is a distinctive characteristic of the genus *Saccharomyces*, which was acquired very late in the evolution of fungi.

Discussion

TGN is the main cargo sorting station in eukaryotic cells. At this location, and with the help of several cargo adaptor complexes, decisions for the delivery of proteins to the different cellular compartments are made (Guo *et al.* 2014). One of these cargo adaptors is exomer, a heterotetrameric complex that is conserved across fungi with no known metazoan homologs (Trautwein *et al.* 2006; Paczkowski *et al.* 2012). According to studies performed using Chs3 as an exomer-dependent cargo model, exomer is thought to mainly interact with cargos through the ChAPs (Rockenbauch *et al.* 2012; Weiskoff and Fromme 2014). These studies identified the ChAP Chs6 as the specific adaptor for this cargo. However, while Chs3 is a well-conserved protein across fungi, Chs6 is not, appearing relatively late in evolution between the Saccharomycotina clade ((Roncero *et al.* 2016) and Figure 2).

This calls into question our current model that regards exomer as a dedicated cargo adaptor.

The results reported in this work support the idea that exomer is an evolutionarily ancient complex, and that some of its functions have been delineated along evolution as the number of ChAPs increased among some fungal groups.

Exomer, a single fungal complex diversified along Saccharomycotina evolution

Our extensive search for exomer components across the fungi kingdom identified a single Chs5 protein in all fungi, but a variable number of ChAPs members. Interestingly, the divergence of ChAPs correlates with the evolutionary history of fungi through a single duplication event from the single ChAPs ancestor, Bch1, early after the branching of the Saccharomycotina group. This was followed by a much later second duplication event associated with the WGD extensively reported for the *Saccharomyces* genus (Wang *et al.* 2009). Moreover, no loss of any of the ChAPs was detected among the different groups, except for *Microsporidia*. This highlights the ancestral significance of exomer and also the potential conservation of the functions associated with exomer. A specialization of ChAPs throughout evolution fits nicely with the current model for exomer assembly. The oldest ChAP, Bch1, seems to be the most efficient in assembling exomer complexes at the TGN, a function partially retained by its close homolog Bud7 (Huranova *et al.* 2016). Accordingly, Bch1 is the ChAP protein

with the largest capacity to promote the membrane remodeling activity associated with exomer *in vitro* (Paczkowski and Fromme 2014). By contrast, Chs6 presents a more specialized function such as a dedicated cargo adaptor (Paczkowski and Fromme 2014). Moreover, our results indicate that Bch2 could have acquired distinctive characteristics owing to the late incorporation of a specific region within its C-terminal domain.

This model raises the significant biological question of whether the role of exomer as a cargo adaptor is evolutionarily conserved. If this is not the case, then what is the conserved function of exomer?

Exomer probably has an ancestral role in the intracellular transport of multiple TM proteins

The *S. cerevisiae* exomer mutants showed additional phenotypic traits that were not associated with known cargos such as sensitivity to alkali metals, hygromycin, or ammonium. Sensitivity to sodium and lithium in *S. cerevisiae* has been recently associated with defects in *Ena1*, a protein that behaves as a nonconventional cargo for exomer (Anton *et al.* 2017). Interestingly, the *Klchs5Δ* and double *Klbch1Δ chs6Δ* mutants also showed lithium sensitivity, but neither of the individual ChAPs mutants, *Klbch1Δ* or *Klchs6Δ*, exhibited this phenotype, clearly indicating functional redundancy between both ChAPs. Similar results were obtained for the sensitivity to hygromycin. However, in *S. cerevisiae* there is limited redundancy between *Chs6/Bch2* and *Bch1/Bud7* pairs based on the different phenotypes exhibited by the double mutants, suggesting a functional specialization of ChAPs along the evolutionary transit between the clades represented by *S. cerevisiae* and *K. lactis*.

The results obtained with respect to ammonium toxicity, although more difficult to interpret, point in the same direction. The absence of the *Bch1/Bud7* pair would be directly responsible for ammonium toxicity in *S. cerevisiae*, with the *Chs6/Bch2* pair playing a minor role. The *K. lactis chs5Δ* mutant was insensitive to ammonium but did show much reduced growth on YES medium. This effect was probably due to a defective intake of external amino acids, since this effect was reversed when the media was supplemented with additional nitrogen sources. This phenotype is probably linked to the ammonium toxicity observed for *S. cerevisiae*, because it has been shown to be ameliorated by the extrusion of intracellular amino acids through the *Ssy1-Ptr3-Ssy5* (SPS) sensing pathway induced amino acid transporters (Hess *et al.* 2006). Defective transport of amino acids in the exomer mutants could be responsible for the ammonium toxicity in *S. cerevisiae*, and also for the defective use of amino acids as a nitrogen source in *K. lactis*. Moreover, the restoration of growth on YES medium, produced by Asp or Glu in *K. lactis*, was only achieved when one ChAP was present, a clear indication that the use of these amino acids depends on a functional exomer, which highlights the functional redundancy between both ChAPs in *K. lactis*. At present, it is unclear whether these exomer-associated defects are due to a defective transport of specific amino acid permeases to the PM or a more general defect in the SPS-sensing system.

Interestingly, the exomer mutants from all the different organisms tested share a slight sensitivity to rapamycin. This phenotype is easily associated with a defective use of nitrogen sources that might explain the evolutionary conservation of exomer across fungi and provides the basis for a more thorough search regarding the ancestral molecular role of exomer.

The unique properties of exomer as a cargo adaptor of Chs3 in *S. cerevisiae*

Exomer has been defined as a cargo adaptor in *S. cerevisiae* owing to the identification of three cargos—*Chs3*, *Fus1* and *Pin2*—which depend on their interaction with exomer for arrival at the PM (Trautwein *et al.* 2006; Barfield *et al.* 2009; Ritz *et al.* 2014). However, only *Chs3* has been clearly shown to depend on the dedicated ChAP protein *Chs6* for its interaction with exomer (Rockenbauch *et al.* 2012). Based on this, the *Scchs5Δ* and *Scchs6Δ* mutants share strongly reduced chitin levels and CW resistance (Roncero 2002). However, deletion of the common exomer component *Chs5* in *U. maydis*, *C. albicans*, or *K. lactis* did not produce a significant reduction in chitin synthesis, despite the fact that the *Chs3* homologs of *U. maydis* and *C. albicans* are evolutionarily conserved and have been shown to be responsible for most chitin synthesis in these organisms (Mio *et al.* 1996; Weber *et al.* 2006). Thus, this result argues against a general role of exomer as a cargo adaptor in fungi. *Chs6* acts at the exomer as a cargo adaptor for *ScChs3* by interacting directly with its C-terminal cytosolic domain (Rockenbauch *et al.* 2012). However, the replacement of the C-terminal region of *ScChs3* by its counterpart region from *CaChs3* led to a protein that is not exported from TGN, probably due to its inability to interact with *Chs6*. Interestingly, the C-terminal region of *Chs3* is not conserved across fungi, suggesting that interaction between *Chs3* and exomer could have been developed late along Saccharomycotina evolution, which is in concordance with a late specialization of the members of the ChAPs family after the WGD.

However, this does not explain the absolute requirement of exomer for *ScChs3* trafficking to the PM. An additional characteristic of all known exomer cargos is their interaction with the AP-1 complex. Moreover, *ScChs3* interacts with AP-1 through a distinct region on its N-terminal cytosolic domain (Starr *et al.* 2012; Weiskoff and Fromme 2014). This region is poorly conserved across fungi, and the replacement of the *ScChs3* N-terminal region by the corresponding region from *CaChs3* produced a chimeric protein that interacted poorly with AP-1 based on phenotypic analysis. These results suggest that *CaChs3* interacts poorly with exomer and AP-1 complexes. The *in vivo* results obtained in *C. albicans* are also consistent with this interpretation, because the exomer mutant *Cachs5Δ* shows a reduced polarization of *CaChs3* resulting in a delocalized deposition of chitin. This situation is similar to that described for the *S. cerevisiae chs5Δ aps1Δ* double mutant, and thus is fully compatible with the absence of an *in vivo* interaction of *CaChs3* with exomer and AP-1 complexes in *C. albicans* cells.

Pin2 is another *bona fide* cargo of exomer in *S. cerevisiae*, for which *Bch2* is the probable cargo adaptor (Ritz *et al.*

2014; Anne Spang, unpublished results); therefore, it would be interesting to test our model using a different cargo. Unfortunately, *Pin2* is poorly conserved across fungi, making it an unsuitable experimental model. Nonetheless, our results strongly support a model in which the role of exomer as cargo adaptor for *Chs3* has evolved in *S. cerevisiae* linked to the engagement of AP-1 in the transport of *Chs3*.

The results presented within this paper recapitulate the evolutionary story of exomer and highlight its progressive specialized role as a cargo adaptor along the Saccharomycotina after the WGD event, a process that is compatible with the maintenance of its ancestral functions in the transport of diverse TM proteins. This model is fully compatible with the role proposed for the most ancestral ChAP, *Bch1*, in vesicle generation at the TGN (Paczkowski and Fromme 2014), and the absence of any known cargos for this protein or its close relative *Bud7*. Moreover, it has not been possible to identify any role for exomer as a cargo adaptor in *C. albicans* and *K. lactis*, once more indicating that this functional specialization most probably occurred very late. The absence of any relevant phenotypes for the exomer mutants of *U. maydis* and *C. albicans* still remains intriguing, and raises questions concerning the most ancestral role of exomer. This would most likely become relevant during stressful conditions, as has been recently reported for *S. pombe* (Hoya *et al.* 2017). However, fungi are adapted to very different ecological niches, which would require additional efforts to identify common stressful conditions for the characterization of the phenotypes associated with the absence of exomer in different fungi.

Acknowledgments

We thank Emma Keck for editing the English, A. Spang and J. Ariño for the many useful discussions that took place throughout this work, R. Valle for her technical assistance at the Roncero Laboratory, S. Chumpen for her help with the overexpression screen, and especially technical help from J. Perez, C. R. Vazquez, and J. J. Heinisch on the work carried out with *U. maydis*, *C. albicans*, and *K. lactis*, respectively. C.A. is supported by a University of Salamanca predoctoral fellowship. C.R. was supported by grant SA073U14 from the Regional Government of Castile and Leon, and by grant BFU2013-48582-C2-1-P from the Comision Interministerial de Ciencia y Tecnologia/Fondo Europeo de Desarrollo Regional Spanish program. J.V.T. is a career researcher at Consejo Nacional de Investigaciones Científicas y Tecnológicas, Argentina, and is supported by grant PICT 2013-0288 from the Agencia Nacional de Promoción Científica y Tecnológica, Argentina.

Literature Cited

Anton, C., B. Zanolari, I. Arcones, C. Wang, J. M. Mulet *et al.*, 2017 Involvement of the exomer complex in the polarized transport of *Ena1* required for *Saccharomyces cerevisiae* survival against toxic cations. *Mol. Biol. Cell* 28: 3672–3685. <https://doi.org/10.1091/mbc.E17-09-0549>

Arcones, I., and C. Roncero, 2016 Monitoring chitin deposition during septum assembly in budding yeast. *Methods Mol. Biol.* 1369: 59–72. https://doi.org/10.1007/978-1-4939-3145-3_5

Arcones, I., C. Sacristán, and C. Roncero, 2016 Maintaining proteome homeostasis: early and late endosomal dual recycling for the maintenance of intracellular pools of the plasma membrane protein *Chs3*. *Mol. Biol. Cell* 27: 4021–4032. <https://doi.org/10.1091/mbc.E16-04-0239>

Banuet, F., and I. Herskowitz, 1989 Different alleles of *Ustilago maydis* are necessary for maintenance of filamentous growth but not for meiosis. *Proc. Natl. Acad. Sci. USA* 86: 5878–5882. <https://doi.org/10.1073/pnas.86.15.5878>

Barfield, R. M., J. C. Fromme, and R. Schekman, 2009 The exomer coat complex transports *Fus1p* to the plasma membrane via a novel plasma membrane sorting signal in yeast. *Mol. Biol. Cell* 20: 4985–4996. <https://doi.org/10.1091/mbc.E09-04-0324>

Barlow, L. D., J. B. Dacks, and J. Wideman, 2014 From all to (nearly) none. *Cell. Logist.* 4: e28114. <https://doi.org/10.4161/cl.28114>

Calderón-Noreña, D. M., A. González-Novo, S. Orellana-Muñoz, P. Gutiérrez-Escribano, Y. Arnáiz-Pita *et al.*, 2015 A single nucleotide polymorphism uncovers a novel function for the transcription factor *Ace2* during *Candida albicans* hyphal development. *PLoS Genet.* 11: e1005152. <https://doi.org/10.1371/journal.pgen.1005152>

Carlson, M., and D. Botstein, 1982 Two differentially regulated mRNAs with different 5' ends encode secreted and intracellular forms of yeast invertase. *Cell* 28: 145–154. [https://doi.org/10.1016/0092-8674\(82\)90384-1](https://doi.org/10.1016/0092-8674(82)90384-1)

Copic, A., T. L. Starr, and R. Schekman, 2007 *Ent3p* and *Ent5p* exhibit cargo-specific functions in trafficking proteins between the trans-Golgi network and the endosomes in yeast. *Mol. Biol. Cell* 18: 1803–1815. <https://doi.org/10.1091/mbc.E06-11-1000>

Daboussi, L., G. Costaguta, and G. S. Payne, 2012 Phosphoinositide-mediated clathrin adaptor progression at the trans-Golgi network. *Nat. Cell Biol.* 14: 239–248. <https://doi.org/10.1038/ncb2427>

Enloe, B., A. Diamond, and A. P. Mitchell, 2000 A single-transformation gene function test in diploid *Candida albicans*. *J. Bacteriol.* 182: 5730–5736. <https://doi.org/10.1128/JB.182.20.5730-5736.2000>

Gola, S., R. Martin, A. Walther, A. Dünkler, and J. Wendland, 2003 New modules for PCR-based gene targeting in *Candida albicans*: rapid and efficient gene targeting using 100 bp of flanking homology region. *Yeast* 20: 1339–1347. <https://doi.org/10.1002/yea.1044>

Goldstein, A. L., and J. H. McCusker, 1999 Three new dominant drug resistance cassettes for gene disruption in *Saccharomyces cerevisiae*. *Yeast* 15: 1541–1553. [https://doi.org/10.1002/\(SICI\)1097-0061\(199910\)15:14<1541::AID-YEA476>3.0.CO;2-K](https://doi.org/10.1002/(SICI)1097-0061(199910)15:14<1541::AID-YEA476>3.0.CO;2-K)

Grigoriev, I., R. Nikitin, S. Haridas, A. Kuo, R. Ohm *et al.*, 2014 MycoCosm portal: gearing up for 1000 fungal genomes. *Nucleic Acids Res.* 42: D699–D704. <https://doi.org/10.1093/nar/gkt1183>

Guo, Y., D. W. Sirkis, and R. Schekman, 2014 Protein sorting at the trans-Golgi network. *Annu. Rev. Cell Dev. Biol.* 30: 169–206. <https://doi.org/10.1146/annurev-cellbio-100913-013012>

Heinisch, J. J., U. Buchwald, A. Gottschlich, N. Heppeler, and R. Rodicio, 2010 A tool kit for molecular genetics of *Kluyveromyces lactis* comprising a congenic strain series and a set of versatile vectors. *FEMS Yeast Res.* 10: 333–342. <https://doi.org/10.1111/j.1567-1364.2009.00604.x>

Hess, D. C., W. Lu, J. D. Rabinowitz, and D. Botstein, 2006 Ammonium toxicity and potassium limitation in yeast. *PLoS Biol.* 4: e351. <https://doi.org/10.1371/journal.pbio.0040351>

Hoya, M., F. Yanguas, S. Moro, C. Prescianotto-Baschong, C. Doncel *et al.*, 2017 Traffic through the trans-Golgi network and the endosomal system requires collaboration between exomer and clathrin adaptors in fission yeast. *Genetics* 205: 673–690. <https://doi.org/10.1534/genetics.116.193458>

- Huranova, M., G. Muruganandam, M. Weiss, and A. Spang, 2016 Dynamic assembly of the exomer secretory vesicle cargo adaptor subunits. *EMBO Rep.* 17: 202–219. <https://doi.org/10.15252/embr.201540795>
- Jimenez, C., C. Sacristan, M. I. Roncero, and C. Roncero, 2010 Amino acid divergence between the CHS domain contributes to the different intracellular behaviour of Family II fungal chitin synthases in *Saccharomyces cerevisiae*. *Fungal Genet. Biol.* 47: 1034–1043. <https://doi.org/10.1016/j.fgb.2010.08.013>
- Lam, K. K., M. Davey, B. Sun, A. F. Roth, N. G. Davis *et al.*, 2006 Palmitoylation by the DHHC protein Pfa4 regulates the ER exit of Chs3. *J. Cell Biol.* 174: 19–25. <https://doi.org/10.1083/jcb.200602049>
- Lenardon, M. D., S. A. Milne, H. M. Mora-Montes, F. A. Kaffarnik, S. C. Peck *et al.*, 2010a Phosphorylation regulates polarisation of chitin synthesis in *Candida albicans*. *J. Cell Sci.* 123: 2199–2206. <https://doi.org/10.1242/jcs.060210>
- Lenardon, M. D., C. A. Munro, and N. A. Gow, 2010b Chitin synthesis and fungal pathogenesis. *Curr. Opin. Microbiol.* 13: 416–423. <https://doi.org/10.1016/j.mib.2010.05.002>
- Longtine, M. S., A. McKenzie, D. J. Demarini, N. G. Shah, A. Wach *et al.*, 1998 Additional modules for versatile and economical PCR-based gene deletion and modification in *Saccharomyces cerevisiae*. *Yeast* 14: 953–961. [https://doi.org/10.1002/\(SICI\)1097-0061\(199807\)14:10<953::AID-YEA293>3.0.CO;2-U](https://doi.org/10.1002/(SICI)1097-0061(199807)14:10<953::AID-YEA293>3.0.CO;2-U)
- Maresova, L., and H. Sychrova, 2005 Physiological characterization of *Saccharomyces cerevisiae kha1* deletion mutants. *Mol. Microbiol.* 55: 588–600. <https://doi.org/10.1111/j.1365-2958.2004.04410.x>
- Markovich, S., A. Yekutieli, I. Shalit, Y. Shadkhan, and N. Osherov, 2004 Genomic approach to identification of mutations affecting caspofungin susceptibility in *Saccharomyces cerevisiae*. *Antimicrob. Agents Chemother.* 48: 3871–3876. <https://doi.org/10.1128/AAC.48.10.3871-3876.2004>
- Mio, T., T. Yabe, M. Sudoh, Y. Satoh, T. Nakajima *et al.*, 1996 Role of three chitin synthase genes in the growth of *Candida albicans*. *J. Bacteriol.* 178: 2416–2419. <https://doi.org/10.1128/jb.178.8.2416-2419.1996>
- Paczkowski, J. E., and J. C. Fromme, 2014 Structural basis for membrane binding and remodeling by the exomer secretory vesicle cargo adaptor. *Dev. Cell* 30: 610–624. <https://doi.org/10.1016/j.devcel.2014.07.014>
- Paczkowski, J. E., B. C. Richardson, A. M. Strassner, and J. C. Fromme, 2012 The exomer cargo adaptor structure reveals a novel GTPase-binding domain. *EMBO J.* 31: 4191–4203. <https://doi.org/10.1038/emboj.2012.268>
- Parsons, A. B., R. L. Brost, H. Ding, Z. Li, C. Zhang *et al.*, 2004 Integration of chemical-genetic and genetic interaction data links bioactive compounds to cellular target pathways. *Nat. Biotechnol.* 22: 62–69. <https://doi.org/10.1038/nbt919>
- Rippert, D., K. Backhaus, R. Rodicio, and J. J. Heinisch, 2017 Cell wall synthesis and central carbohydrate metabolism are interconnected by the SNF1/Mig1 pathway in *Kluyveromyces lactis*. *Eur. J. Cell Biol.* 96: 70–81. <https://doi.org/10.1016/j.ejcb.2016.12.004>
- Ritz, A. M., M. Trautwein, F. Grassinger, and A. Spang, 2014 The prion-like domain in the exomer-dependent cargo Pin2 serves as a trans-Golgi retention motif. *Cell Rep.* 7: 249–260. <https://doi.org/10.1016/j.celrep.2014.02.026>
- Rockenbauch, U., A. M. Ritz, C. Sacristan, C. Roncero, and A. Spang, 2012 The complex interactions of Chs5p, the ChAPs, and the cargo Chs3p. *Mol. Biol. Cell* 23: 4402–4415. <https://doi.org/10.1091/mbc.E11-12-1015>
- Roncero, C., 2002 The genetic complexity of chitin synthesis in fungi. *Curr. Genet.* 41: 367–378. <https://doi.org/10.1007/s00294-002-0318-7>
- Roncero, C., A. Sanchez-Diaz, and M. H. Valdivieso, 2016 Chitin synthesis and fungal morphogenesis, pp. 167–190 in *The Mycota* III. *Biochemistry and Molecular Biology*, edited by D. Hoffmeister. Springer-Verlag, Heidelberg, Germany. https://doi.org/10.1007/978-3-319-27790-5_9
- Rose, M. D., F. Winston, and P. Hieter, 1990 *Methods in Yeast Genetics: A Laboratory Course Manual*. Cold Spring Harbor Laboratory Press, Cold Spring Harbor, NY.
- Sacristan, C., A. Reyes, and C. Roncero, 2012 Neck compartmentalization as the molecular basis for the different endocytic behaviour of Chs3 during budding or hyperpolarized growth in yeast cells. *Mol. Microbiol.* 83: 1124–1135. <https://doi.org/10.1111/j.1365-2958.2012.07995.x>
- Sacristan, C., J. Manzano-Lopez, A. Reyes, A. Spang, M. Muniz *et al.*, 2013 Dimerization of the chitin synthase Chs3 is monitored at the Golgi and affects its endocytic recycling. *Mol. Microbiol.* 90: 252–266.
- Sanchatjate, S., and R. Schekman, 2006 Chs5/6 complex: a multi-protein complex that interacts with and conveys chitin synthase III from the trans-Golgi network to the cell surface. *Mol. Biol. Cell* 17: 4157–4166. <https://doi.org/10.1091/mbc.E06-03-0210>
- Santos, B., and M. Snyder, 1997 Targeting of chitin synthase 3 to polarized growth sites in yeast requires Chs5p and Myo2p. *J. Cell Biol.* 136: 95–110. <https://doi.org/10.1083/jcb.136.1.95>
- Santos, B., and M. Snyder, 2003 Specific protein targeting during cell differentiation: polarized localization of Fus1p during mating depends on Chs5p in *Saccharomyces cerevisiae*. *Eukaryot. Cell* 2: 821–825. <https://doi.org/10.1128/EC.2.4.821-825.2003>
- Sanz, M., L. Carrano, C. Jimenez, G. Candiani, J. A. Trilla *et al.*, 2005 *Candida albicans* strains deficient in *CHS7*, a key regulator of chitin synthase III, exhibit morphogenetic alterations and attenuated virulence. *Microbiology* 151: 2623–2636. <https://doi.org/10.1099/mic.0.28093-0>
- Sato, M., S. Dhut, and T. Toda, 2005 New drug-resistant cassettes for gene disruption and epitope tagging in *Schizosaccharomyces pombe*. *Yeast* 22: 583–591. <https://doi.org/10.1002/yea.1233>
- Schaub, Y., A. Dünkler, A. Walther, and J. Wendland, 2006 New pFA-cassettes for PCR-based gene manipulation in *Candida albicans*. *J. Basic Microbiol.* 46: 416–429. <https://doi.org/10.1002/jobm.200510133>
- Schlacht, A., E. K. Herman, M. J. Klute, M. C. Field, and J. B. Dacks, 2014 Missing pieces of an ancient puzzle: evolution of the eukaryotic membrane-trafficking system. *Cold Spring Harb. Perspect. Biol.* 6: a016048. <https://doi.org/10.1101/cshperspect.a016048>
- Spang, A., 2015 The road not taken: less traveled roads from the TGN to the plasma membrane. *Membranes (Basel)* 5: 84–98. <https://doi.org/10.3390/membranes5010084>
- Starr, T. L., S. Pagant, C. W. Wang, and R. Schekman, 2012 Sorting signals that mediate traffic of chitin synthase III between the TGN/endosomes and to the plasma membrane in yeast. *PLoS One* 7: e46386.
- Stuckey, S., K. Mukherjee, and F. Storici, 2011 In vivo site-specific mutagenesis and gene collage using the delitto perfetto system in yeast *Saccharomyces cerevisiae*. *Methods Mol. Biol.* 745: 173–191. https://doi.org/10.1007/978-1-61779-129-1_11
- Terfrüchte, M., B. Joehnk, R. Fajardo-Somera, G. H. Braus, M. Riquelme *et al.*, 2014 Establishing a versatile Golden Gate cloning system for genetic engineering in fungi. *Fungal Genet. Biol.* 62: 1–10. <https://doi.org/10.1016/j.fgb.2013.10.012>
- Thompson, J. R., E. Register, J. Curotto, M. Kurtz, and R. Kelly, 1998 An improved protocol for the preparation of yeast cells for transformation by electroporation. *Yeast* 14: 565–571. [https://doi.org/10.1002/\(SICI\)1097-0061\(19980430\)14:6<565::AID-YEA251>3.0.CO;2-B](https://doi.org/10.1002/(SICI)1097-0061(19980430)14:6<565::AID-YEA251>3.0.CO;2-B)
- Tonikian, R., X. Xin, C. P. Toret, D. Gfeller, C. Landgraf *et al.*, 2009 Bayesian modeling of the yeast SH3 domain interactome predicts spatiotemporal dynamics of endocytosis proteins. *PLoS Biol.* 7: e1000218. <https://doi.org/10.1371/journal.pbio.1000218>

- Trautwein, M., C. Schindler, R. Gauss, J. Dengjel, E. Hartmann *et al.*, 2006 Arf1p, Chs5p and the ChAPs are required for export of specialized cargo from the Golgi. *EMBO J.* 25: 943–954. <https://doi.org/10.1038/sj.emboj.7601007>
- Trilla, J. A., A. Duran, and C. Roncero, 1999 Chs7p, a new protein involved in the control of protein export from the endoplasmic reticulum that is specifically engaged in the regulation of chitin synthesis in *Saccharomyces cerevisiae*. *J. Cell Biol.* 145: 1153–1163. <https://doi.org/10.1083/jcb.145.6.1153>
- Trueheart, J., J. D. Boeke, and G. R. Fink, 1987 Two genes required for cell fusion during yeast conjugation: evidence for a pheromone-induced surface protein. *Mol. Cell. Biol.* 7: 2316–2328. <https://doi.org/10.1128/MCB.7.7.2316>
- Tsukuda, T., S. Carleton, S. Fotheringham, and W. K. Holloman, 1988 Isolation and characterization of an autonomously replicating sequence from *Ustilago maydis*. *Mol. Cell. Biol.* 8: 3703–3709. <https://doi.org/10.1128/MCB.8.9.3703>
- Valdivia, R. H., D. Baggot, J. S. Chuang, and R. Schekman, 2002 The yeast Clathrin adaptor protein complex 1 is required for the efficient retention of a subset of late Golgi membrane proteins. *Dev. Cell* 2: 283–294. [https://doi.org/10.1016/S1534-5807\(02\)00127-2](https://doi.org/10.1016/S1534-5807(02)00127-2)
- Wang, C. W., S. Hamamoto, L. Orci, and R. Schekman, 2006 Exomer: a coat complex for transport of select membrane proteins from the trans-Golgi network to the plasma membrane in yeast. *J. Cell Biol.* 174: 973–983. <https://doi.org/10.1083/jcb.200605106>
- Wang, H., Z. Xu, L. Gao, and B. Hao, 2009 A fungal phylogeny based on 82 complete genomes using the composition vector method. *BMC Evol. Biol.* 9: 195. <https://doi.org/10.1186/1471-2148-9-195>
- Weber, I., D. Assmann, E. Thines, and G. Steinberg, 2006 Polar localizing class V myosin chitin synthases are essential during early plant infection in the plant pathogenic fungus *Ustilago maydis*. *Plant Cell* 18: 225–242. <https://doi.org/10.1105/tpc.105.037341>
- Weiskoff, A. M., and J. C. Fromme, 2014 Distinct N-terminal regions of the exomer secretory vesicle cargo Chs3 regulate its trafficking itinerary. *Front. Cell Dev. Biol.* 2: 47. <https://doi.org/10.3389/fcell.2014.00047>
- Ziman, M., J. S. Chuang, M. Tsung, S. Hamamoto, and R. Schekman, 1998 Chs6p-dependent anterograde transport of Chs3p from the chitosome to the plasma membrane in *Saccharomyces cerevisiae*. *Mol. Biol. Cell* 9: 1565–1576. <https://doi.org/10.1091/mbc.9.6.1565>

Communicating editor: J. Heitman